

Theoretical Study on Monoligated Pd-Catalyzed Cross-Coupling Reactions of Aryl Chlorides and Bromides

Zhe Li,[†] Yao Fu,^{*,†} Qing-Xiang Guo,[†] and Lei Liu^{*,‡}

Department of Chemistry, University of Science and Technology of China, Hefei 230026, China, and
Department of Chemistry, Tsinghua University, Beijing 100084, China

Received October 24, 2007

The mechanism of oxidative addition of aryl halides to Pd(PR₃)₂ (R = Me, Et, *i*Pr, *t*Bu, Ph) was investigated by using density functional theory methods enhanced with a polarized continuum solvation model. Different reaction pathways were discussed on the basis of Gibbs free-energy profiles in a tetrahydrofuran solution. The calculations indicated that monophosphine PdPR₃ was catalytically more active than bisphosphine Pd(PR₃)₂ for oxidative addition. However, among different PR₃ ligands (R = Me, Et, *i*Pr, *t*Bu, Ph), the free-energy barriers for oxidative addition to PdPR₃ did not change significantly (i.e., less than 2 kcal/mol). This gave rise to an important question: why was P(*t*-Bu)₃ the only catalytically active ligand toward aryl chlorides among the above five ligands? It was proposed on the basis of the calculated data that the difference of the dissociation energies from PdL₂ to PdL and L (L = ligand) between the various PR₃ ligands dictated their dissimilar reactivity in oxidative addition.

1. Introduction

Pd-catalyzed cross-coupling reactions of aryl (and alkenyl) halides such as Heck olefination, Suzuki coupling, Stille coupling, and Buchwald–Hartwig amination are indispensable tools in modern organic synthesis.¹ Until recently, nearly all reports of Pd-catalyzed couplings described the use of aryl bromides and iodides as substrates, whereas the more readily available aryl chlorides were noticeably uncommon partners. The poor reactivity of aryl chlorides in Pd catalysis has often been explained as a result of the reluctance by aryl chlorides to oxidatively add to Pd⁰ centers, a critical initial step in Pd-catalyzed coupling reactions. To overcome this problem, many recent studies have been directed toward the development of Pd catalysts based on bulky and electron-rich phosphanes (as well as carbenes), where some catalysts have been discovered to be capable of accomplishing cross-couplings of unactivated aryl chlorides.² In spite of these achievements, there remains a strong need for further improvement in terms of the catalyst price, scope, selectivity, and efficiency. This task requires us not only to continue the experimental screening of new ligands and reaction conditions³ but also to gain a rational understanding of why each certain Pd catalyst can or cannot activate aryl chlorides.

Previously, the enhanced reactivity observed with the Pd catalysts carrying bulky and electron-rich ligands was attributed to the formation of monoligated [PdL] species, which were believed to undergo oxidative addition reactions more readily

than [PdL₂].⁴ This argument has received some support from the mechanistic studies by Hartwig et al.⁵ and Brown et al.,⁶ where it was shown that Pd complexes with bulky phosphines (such as *Pt*Bu₃) underwent oxidative addition with aryl halides by a dissociative mechanism. Furthermore, by treating the phenyl halides either with [Pd(PR₃)₂] or with mixtures of [Pd(dba)₂] and 1 equiv of the corresponding phosphine, Hartwig and co-workers recently isolated a series of tricoordinated Pd^{II} compounds with the general formula [Pd(Ph)X(PR₃)] [PR₃ = PAd*t*Bu₂, *Pt*Bu₃, or (Ph₅Fc)*Pt*Bu₂].⁷ These tricoordinated Pd^{II} compounds further supported the possibility that aryl halides tend to oxidatively add to monoligated Pd⁰ complexes carrying bulky phosphine ligands.

Evidently, the above mechanistic studies have provided important insights into the aryl chloride activation problem. Nonetheless, there still remain several significant questions that have not been answered by any previous study: (1) To what extent can a monoligated Pd complex outperform a bisligated one in the oxidative addition step? (2) How bulky and how electron-rich does a monoligated phosphine ligand need to be in order to accomplish aryl chloride activation? Answers to these

(3) Very recent examples: (a) Fernandez-Rodriguez, M. A.; Shen, Q.; Hartwig, J. F. *Chem.—Eur. J.* **2006**, *12*, 7782. (b) Yin, L.; Zhang, Z.-H.; Wang, Y.-M. *Tetrahedron* **2006**, *62*, 9359. (c) Xie, X.; Zhang, T. Y.; Zhang, Z. *J. Org. Chem.* **2006**, *71*, 6522. (d) Christmann, U.; Pantazis, D. A.; Benet-Buchholz, J.; McGrady, J. E.; Maseras, F.; Vilar, R. *J. Am. Chem. Soc.* **2006**, *128*, 6376. (e) Dai, Q.; Gao, W.; Liu, D.; Kapes, L. M.; Zhang, X. *J. Org. Chem.* **2006**, *71*, 3928. (f) Ackermann, L.; Gschrei, C. J.; Althammer, A.; Riederer, M. *Chem. Commun.* **2006**, 1419. (g) Yi, C.; Hua, R. *Tetrahedron Lett.* **2006**, *47*, 2573. (h) Marion, N.; Navarro, O.; Mei, J.; Stevens, E. D.; Scott, N. M.; Nolan, S. P. *J. Am. Chem. Soc.* **2006**, *128*, 4101. (i) Tewari, A.; Hein, M.; Zapf, A.; Beller, M. *Tetrahedron* **2005**, *61*, 9705. (j) Song, C.; Ma, Y.; Chai, Q.; Ma, C.; Jiang, W.; Andrus, M. B. *Tetrahedron* **2005**, *61*, 7438. (k) Barder, T. E.; Walker, S. D.; Martinelli, J. R.; Buchwald, S. L. *J. Am. Chem. Soc.* **2005**, *127*, 4685.

(4) Christmann, U.; Vilar, R. *Angew. Chem., Int. Ed.* **2005**, *44*, 366.

(5) Hartwig, J. F. *Angew. Chem., Int. Ed.* **1998**, *37*, 2046.

(6) Galardon, E.; Ramdeehul, S.; Brown, J. M.; Cowley, A.; Hii, K. K.; Jutand, A. *Angew. Chem., Int. Ed.* **2002**, *41*, 1760.

(7) (a) Stambuli, J. P.; Buehl, M.; Hartwig, J. F. *J. Am. Chem. Soc.* **2002**, *124*, 9346. (b) Stambuli, J. P.; Incarvito, C. D.; Buehl, M.; Hartwig, J. F. *J. Am. Chem. Soc.* **2004**, *126*, 1184. (c) Yamashita, M.; Hartwig, J. F. *J. Am. Chem. Soc.* **2004**, *126*, 5344.

* To whom correspondence should be addressed. E-mail: fuyao@ustc.edu.cn (Y.F.), lliu@mail.tsinghua.edu.cn (L.L.).

[†] University of Science and Technology of China.

[‡] Tsinghua University.

(1) Negishi, E. I., Ed. *Handbook of Organopalladium Chemistry for Organic Synthesis*; Wiley-Interscience: New York, 2002.

(2) Articles: (a) Luke, F.; Fu, G. C. *J. Am. Chem. Soc.* **2007**, *129*, 11340. (b) Zhou, J. R.; Fu, G. C. *J. Am. Chem. Soc.* **2003**, *125*, 12527. (c) Littke, A. F.; Dai, C. Y.; Fu, G. C. *J. Am. Chem. Soc.* **2000**, *122*, 4020. (d) Littke, A. F.; Fu, G. C. *Angew. Chem., Int. Ed.* **1999**, *38*, 2411. (e) Littke, A. F.; Fu, G. C. *Angew. Chem., Int. Ed.* **2002**, *41*, 4176. (f) Ackermann, L. *Synthesis* **2006**, 1557. (g) Corbet, J.-P.; Mignani, G. *Chem. Rev.* **2006**, *106*, 2651.

questions are of obvious value to the continuing search for superior Pd catalysts and, therefore, constitute the focal points of our present work. Noteworthy, in a very recent theoretical study on the oxidative addition of PhI to $[\text{Pd}(\text{PPh}_3)_2]$,⁸ Norrby et al. showed that “the most favored oxidative addition is obtained when Pd is coordinated by only the aryl iodide and one additional ligand” despite the fact that PPh_3 is usually not considered as a bulky ligand. This example illustrates the current complication in our understanding of monoligated Pd catalysts, where many mechanistic details need to be investigated in depth.⁹

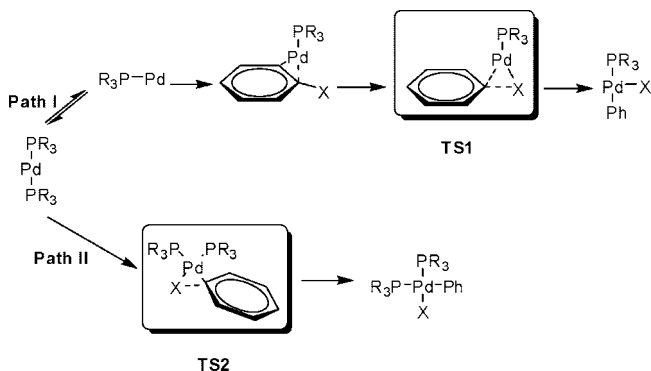
2. Computational Details

All of the calculations were performed with the *Gaussian 03* software.¹⁰ The gas-phase geometries of all compounds were optimized without any constraint by the density functional theory (DFT) method B3PW91¹¹ with the basis set LANL2DZ+p.¹² Polarization functions were added for P ($\xi_d = 0.387$), Cl ($\xi_d = 0.640$), Br ($\xi_d = 0.428$), and Pd ($\xi_f = 1.472$).¹³ Frequency analysis was performed after optimization to verify the minima and transition states.

Single-point energies were then calculated at the PBEPBE¹⁴/BS1 level, where the SDD¹⁵ basis set was augmented by f functions ($\xi_f = 2.203$ and 0.621) for Pd and the 6-31+G* basis set was for other atoms. Note that the B3PW91 method was previously shown to be optimal for geometry optimization of Pd complexes.^{16a} The PBEPBE functional was chosen for the energy calculation because Truhlar et al. showed that this functional could provide accurate energies for transition metals.^{16b}

Gibbs free-energy corrections at 298 K were determined from harmonic frequencies and added to the total electronic energies to get the Gibbs free energies. Subsequently, the gas-phase Gibbs free

Scheme 1. Proposed Mechanism of the Oxidative Addition of PhX (X = Cl, Br) to $[\text{Pd}(\text{P}(\text{R}_3)_2)_2]$



energies were converted to free energies in the tetrahydrofuran (THF) solution. The solvation energies were calculated by the polarized continuum solvation model (PCM) with UAHF radii on the geometries of single points on the PBEPBE/BS1 level. Both the electronic and nonelectronic free energies in solution are added to the gas-phase Gibbs free energies to obtain the free energies in THF. No explicit THF molecules are added to the vacant site of Pd complexes because it was reported that the change of solvents did not have an obvious effect on the rate of oxidative addition.^{7c}

To validate the gas-phase geometries, geometries of some key species were also fully optimized in the THF solution at the B3PW91/LANL2DZ+p level, with the PCM employing UA0 radii. The frequency analysis was carried out in the solution to obtain the correction of the Gibbs free energy.

3. Results

3.1. Proposed Mechanism. We postulate two mechanisms of the oxidative addition reaction (Scheme 1): (1) Path I involves dissociation of one phosphine ligand from $[\text{Pd}^0\text{L}_2]$ to generate the monophosphine complex $[\text{PdL}]$. Then $[\text{PdL}]$ combines with PhX to form the reactant complex $[\text{Pd}(\eta^2\text{-PhX})\text{L}]$.¹⁷ Finally, $[\text{Pd}(\eta^2\text{-PhX})\text{L}]$ undergoes oxidative addition via TS1 and transforms into a tricoordinated Pd complex $[\text{PdL}(\text{Ph})\text{X}]$. (2) Path II involves the direct oxidative addition of PhX to the bisphosphine complex $[\text{PdL}_2]$ via a bisphosphine-containing transition state TS2 to form *cis*- $[\text{PdL}_2(\text{Ph})\text{X}]$.

3.2. Intermediates and Transition States Containing the $\text{P}(\text{tBu})_3$ Ligand. It was reported that $\{\text{Pd}[\text{P}(\text{tBu})_3]_2\}$ is the major species in solution before the oxidative addition step.¹⁸ Accordingly, we choose $\{\text{Pd}[\text{P}(\text{tBu})_3]_2\}$ as the reference point of Gibbs free energies for all of the active species. $\{\text{Pd}[\text{P}(\text{tBu})_3]_2\}$ has a linear geometry with two $\text{P}(\text{tBu})_3$ staggered to each other and a Pd–P bond length of 2.35 Å (Figure 1). The Pd–P bond decreases to 2.24 Å after losing a $\text{P}(\text{tBu})_3$ ligand to form monoligated $\{\text{Pd}[\text{P}(\text{tBu})_3]\}$, showing the strong trans influence of the $\text{P}(\text{tBu})_3$ ligand.¹⁹ The ligand dissociation is endergonic by 19.4 kcal/mol in the THF solution (Table 1, entry 2). The coordinately unsaturated complex $\{\text{Pd}[\text{P}(\text{tBu})_3]\}$ can readily combine with one molecule of PhX to form the reactive complex $\{\text{Pd}(\eta^2\text{-PhX})[\text{P}(\text{tBu})_3]\}$. This process is exergonic by

(8) Ahlquist, M.; Fristrup, P.; Tanner, D.; Norrby, P.-O. *Organometallics* **2006**, *25*, 2066.

(9) Recent progress: (a) Goossen, L. J.; Koley, D.; Hermann, H.; Thiel, W. *Chem. Commun.* **2004**, 2141. (b) Cundari, T. R.; Deng, J. J. *Phys. Org. Chem.* **2005**, 417. (c) Goossen, L. J.; Koley, D.; Hermann, H. L.; Thiel, W. *J. Am. Chem. Soc.* **2005**, *127*, 11102. (d) Kozuch, S.; Amatore, C.; Jutand, A.; Shaik, S. *Organometallics* **2005**, *24*, 2319. (e) Goossen, L. J.; Koley, D.; Hermann, H. L.; Thiel, W. *Organometallics* **2006**, *25*, 54. (f) Shaik, S.; Kozuch, S. *J. Am. Chem. Soc.* **2006**, *128*, 3355. (g) Braga, A. A. C.; Ujaque, G.; Maseras, F. *Organometallics* **2006**, *25*, 3662. (h) Ananikov, V. P.; Musaev, D. G.; Morokuma, K. *Eur. J. Inorg. Chem.* **2007**, 5390.

(10) Frisch, M. J.; Trucks, G. W.; Schlegel, H. B.; et al. *Gaussian 03*, revisions D.01 and B.05; Gaussian, Inc.: Wallingford, CT, and Pittsburgh, PA, 2004.

(11) (a) Becke, A. D. *Phys. Rev. A* **1988**, *38*, 3098. (b) Burke, K.; Perdew, J. P.; Wang, Y.; Dobson, J. F.; Vignale, G.; Das, M. P. *Electronic Density Functional Theory: Recent Progress and New Directions*; Plenum: New York, 1998. (c) Perdew, J. P.; Ziesche, P.; Eschrig, H. *Electronic Structure of Solids '91*; Akademie Verlag: Berlin, 1991. (d) Perdew, J. P.; Chevary, J. A.; Vosko, S. H.; Jackson, K. A.; Pederson, M. R.; Singh, D. J.; Fiolhais, C. *Phys. Rev. B* **1992**, *46*. (e) Perdew, J. P.; Chevary, J. A.; Vosko, S. H.; Jackson, K. A.; Pederson, M. R. D.; Singh, J.; Fiolhais, C. *Phys. Rev. B* **1993**, *48*. (f) Perdew, J. P.; Burke, K.; Wang, Y. *Phys. Rev. B* **1996**, *54*, 16533.

(12) (a) Dunning, T. H., Jr.; Hay, P. J.; Schaefer, H. F., III. *Modern Theoretical Chemistry*; Plenum: New York, 1976; Vol. 3, pp 1–28. (b) Hay, P. J.; Wadt, W. R. *J. Chem. Phys.* **1985**, *82*, 270. (c) Wadt, W. R.; Hay, P. J. *J. Chem. Phys.* **1985**, *82*, 284. (d) Hay, P. J.; Wadt, W. R. *J. Chem. Phys.* **1985**, *82*, 299.

(13) (a) Ehlers, A. W.; Bohme, M.; Dapprich, S.; Gobbi, A.; Hollwarth, A.; Jonas, V.; Kohler, K. F.; Stegmann, R.; Veldkamp, A.; Frenking, G. *Chem. Phys. Lett.* **1993**, *208*, 111. (b) Hollwarth, A.; Bohme, M.; Dapprich, S.; Ehlers, A. W.; Gobbi, A.; Jonas, V.; Kohler, K. F.; Stegmann, R.; Veldkamp, A.; Frenking, G. *Chem. Phys. Lett.* **1993**, *208*, 237.

(14) (a) Perdew, J. P.; Burke, K.; Ernzerhof, M. *Phys. Rev. Lett.* **1996**, *77*, 3865. (b) Perdew, J. P.; Burke, K.; Ernzerhof, M. *Phys. Rev. Lett.* **1997**, *78*, 1396.

(15) (a) Andrae, D.; Haeussermann, U.; Dolg, M.; Stoll, H.; Preuss, H. *Theor. Chim. Acta* **1990**, *77*, 123. (b) Martin, J. M. L.; Sundermann, A. *J. Chem. Phys.* **2001**, *114*, 3408.

(16) (a) Li, Z.; Liu, L.; Fu, Y.; Guo, Q.-X. *THEOCHEM* **2005**, 757, 69. (b) Schultz, N. E.; Zhao, Y.; Truhlar, D. G. *J. Phys. Chem. A* **2005**, *109*, 11127–11143.

(17) (a) Goossen, L. J.; Koley, D.; Hermann, H. L.; Thiel, W. *Organometallics* **2005**, *24*, 2398–2410. (b) Senn, H. M.; Ziegler, T. *Organometallics* **2004**, *23*, 2980.

(18) Barrios-Landeros, F.; Harwig, J. F. *J. Am. Chem. Soc.* **2005**, *127*, 6944.

(19) Spessard, G. O.; Miessler, G. L. *Organometallic Chemistry*; Prentice-Hall, Upper Saddle River, NJ, 1997; pp 140–145.

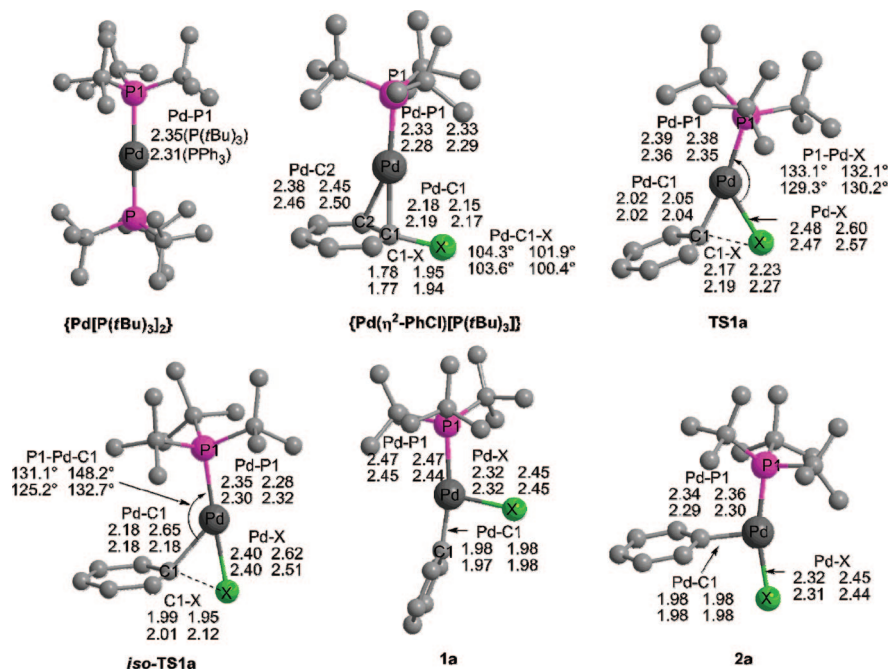


Figure 1. Geometries of the species in path I. The first line of the values of bond lengths and angles belongs to the $P(tBu)_3$ ligand, the second line belongs to the PPh_3 ligand, the first column belongs to $PhCl$, and the second column belongs to $PhBr$.

Table 1. Free Energies of Intermediates and Transition States of Path I with the $P(tBu)_3$ Ligand (kcal/mol)

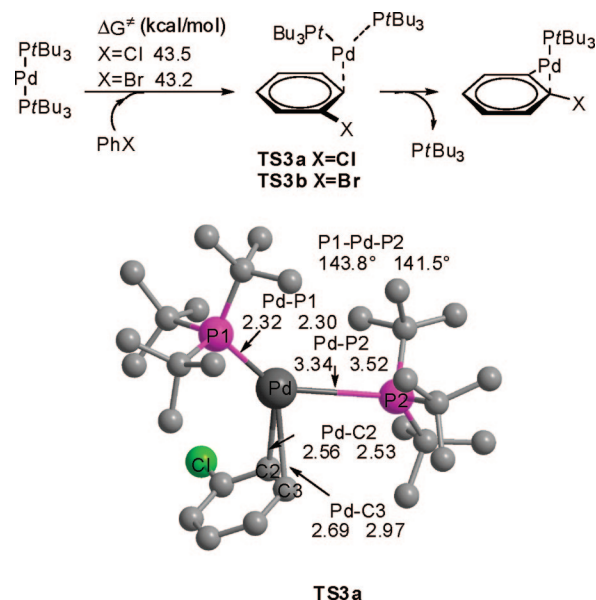
Entry		Free Energy (kcal/mol)
1	$\{Pd[P(tBu)_3]_2\}$	0.0
2	$\{Pd[P(tBu)_3]\}$	19.4
3	$\{Pd(\eta^2-PhCl)[P(tBu)_3]\}$	12.5
4	$\{Pd(\eta^2-PhBr)[P(tBu)_3]\}$	12.2
5	 TS1a	21.3
6	 iso-TS1a	20.9
7	 1a	10.7
8	 2a	-0.8
9	 TS1b	13.0
10	 iso-TS1b	19.3
11	 1b	4.7
12	 2b	-5.3

6.9 and 7.2 kcal/mol for $PhCl$ and $PhBr$, respectively (Table 1, entries 3 and 4). The $Pd-P$ bonds are elongated to 2.33 Å in both $\{Pd(\eta^2-PhCl)[P(tBu)_3]\}$ and $\{Pd(\eta^2-PhBr)[P(tBu)_3]\}$.

Two transition states of the oxidative addition of $PhCl$ to $\{Pd[P(tBu)_3]\}$ are located, $TS1a$ and $iso-TS1a$. The barrier of $TS1a$ is 21.3 kcal/mol, and the barrier of $iso-TS1a$ is 20.9 kcal/mol (Table 1, entries 5 and 6). Although $iso-TS1a$ is favored for $PhCl$, $TS1b$ has a free energy of 13.0 kcal/mol, a value much lower than that of $iso-TS1b$, 19.3 kcal/mol. The free-energy difference between $TS1a$ and $iso-TS1a$ can be rationalized by the fact that $iso-TS1a$ is much earlier on the reaction coordinates than $TS1a$. The $C1-Cl$ bond length of $iso-TS1a$ is 1.99 Å, which is 0.18 Å shorter than the $C1-Cl$ bond of $TS1a$. The longer $C-Cl$ bond in $TS1a$ needs more energy to overcome the large $C-Cl$ bond dissociation enthalpy, leading to a more unstable transition state. However, besides benefitting from the early position on the reaction coordinates, $iso-TS1a$ suffers from the steric repulsion between the phenyl ring and the hydrogen atoms of the $PtBu_3$ ligand. The interplay of the reaction coordinates and steric repulsion determines whether the favored transition state is $TS1a$ or $iso-TS1a$. As to $PhCl$, the barrier of $iso-TS1a$ is lower than that of $TS1a$. In the case of $PhBr$, because of the much lower bond dissociation enthalpy of the $C-Br$ bond than the $C-Cl$ bond and the larger distance between the hydrogen atoms of $PtBu_3$ and the phenyl ring, the free energy of $TS1b$ is lower than that of $iso-TS1b$ by 6.3 kcal/mol. Thus, $TS1b$ is favored in the oxidative addition of $PhBr$ with $\{Pd[P(tBu)_3]\}$.

$TS1a$ leads to product **1a** with a free energy of 10.7 kcal/mol, and $iso-TS1a$ leads to product **2a** with a free energy of -0.8 kcal/mol. The product **2b** of $PhBr$ with $\{Pd[P(tBu)_3]\}$ is also more exergonic than **1b** by 10.0 kcal/mol. There is a vacant spot on **1a**, **2a**, **1b**, and **2b**, which can accept a substrate such as olefin (in the Heck reaction) or organoboronic acid (in the Suzuki reaction). **1a** and **2a** (or **1b** and **2b**) may also isomerize to each other. However, because we intend to focus on the oxidative addition step, we choose not to investigate the isomerization process in detail.

Attempts to locate a bisphosphine transition state of the oxidation of PhX to $Pd(PtBu_3)_2$ always lead to the dissociation of one $PtBu_3$ ligand, presumably because of the large steric effect of the $PtBu_3$ ligand. An η^2 (via the $C_{ipso}-C_{ortho}$ double

Scheme 2. Associative Substitution of the $PtBu_3$ Ligand^a

^a In the graph, the first number of bond lengths and angles belongs to PhCl and the second belongs to PhBr.

bond on the phenyl ring) or σ (via the halide atom) complex of the type $PhX-Pd(PtBu_3)_2$ cannot be found either. However, the transition state of the substitution of PhX to $PtBu_3$ has been successfully found (TS3a and TS3b; Scheme 2). The corresponding energy barriers are 43.5 kcal/mol for PhCl and 43.2 kcal/mol for PhBr. Because these barriers are much higher than the ligand dissociation energy of $PtBu_3$, the formation of reactant complex $[Pd(\eta^2-PhX)L]$ should not undergo this associative pathway.

3.3. Intermediates and Transition States Containing a PPh_3 Ligand. Pd^0 can coordinate four PPh_3 ligands at most, but $[Pd(PPh_3)_3]$ and $[Pd(PPh_3)_2]$ are the major species in solution.²⁰ Theoretical studies by Norrby et al. showed that the concentration of $[Pd(PPh_3)_3]$ should be infinitesimally low.⁸ As a result, we choose $[Pd(PPh_3)_2]$ as the reference point of the free-energy profile. The geometric difference between the corresponding catalytic species of $PtBu_3$ and PPh_3 ligands is trivial; i.e., bond lengths vary by less than 0.1 Å (Figure 1). However, the Gibbs free energies have some interesting differences. The dissociation of one PPh_3 ligand from $[Pd(PPh_3)_2]$ is endergonic by 22.0 kcal/mol (Table 2, entry 2), and this value is 2.6 kcal/mol higher than that of $\{Pd[PtBu_3]\}$. Subsequently, the monophosphine complex $[Pd(PPh_3)]$ coordinates to substrates PhX to form $[Pd(\eta^2-PhX)(PPh_3)]$. The Gibbs free energy of $[Pd(\eta^2-PhCl)(PPh_3)]$ (Table 2, entry 3) is about 2 kcal/mol higher than those of $\{Pd(\eta^2-PhCl)[P(tBu_3)_3]\}$, $\{Pd(\eta^2-PhBr)[P(tBu_3)_3]\}$, and $[Pd(\eta^2-PhBr)(PPh_3)]$.

Different from the case of TS1a, the barrier of transition state TS1c is 23.4 kcal/mol, 0.5 kcal/mol lower than that of iso-TS1c. The barrier of TS1d is 1.3 kcal/mol lower than that of iso-TS1d. As a result, TS1c and TS1d are favored in the oxidative addition to $[Pd(PPh_3)]$. The free energies of the transition states relative to $[PdL_2]$ decrease in the order TS1c (23.4) > iso-TS1a (20.9) > TS1b (15.8) > TS1d (13.0). The products $[Pd(PPh_3)(Ph)Cl]$ (**1c**) and $[Pd(PPh_3)(Ph)Br]$ (**1d**) have free energies of 16.1 and

Table 2. Relative Free Energies of Intermediates of Path I with the PPh_3 Ligand (kcal/mol)

Entry	Structure	Free Energy (kcal/mol)
1	$[Pd(PPh_3)_2]$	0.0
2	$[Pd(PPh_3)]$	22.0
3	$[Pd(\eta^2-PhCl)(PPh_3)]$	15.1
4	$[Pd(\eta^2-PhBr)(PPh_3)]$	12.6
5	TS1c	23.4
6	iso-TS1c	23.9
7	1c	16.1
8	2c	0.5
9	TS1d	15.8
10	iso-TS1d	17.1
11	1d	9.0
12	2d	-3.9

Table 3. Relative Free Energies of Intermediates of Path II with the PPh_3 Ligand (kcal/mol)

Entry	Structure	Free Energy (kcal/mol)
1	TS2c	34.4
2	TS2d	25.0
3	cis- $[Pd(PPh_3)_2(Ph)Cl]$	6.9
4	cis- $[Pd(PPh_3)_2(Ph)Br]$	1.5
5	trans- $[Pd(PPh_3)_2(Ph)Cl]$	-2.4
6	trans- $[Pd(PPh_3)_2(Ph)Br]$	-7.3

9.0 kcal/mol, respectively (Table 2, entries 7 and 11). **2c** and **2d** are again more stable products with free energies of +0.5 and -3.9 kcal/mol, respectively.

Transition states (TS2c and TS2d) of oxidative addition with two PPh_3 ligands are also found. The corresponding free-energy barriers are 34.4 and 25.0 kcal/mol (Table 3, entries 1 and 2), respectively. The geometry of the transition state is tetrahedral (Figure 2), and the Pd-C1 bond (2.12 Å of TS2c and 2.13 Å of TS2d) is about 0.1 Å longer than that of the monophosphine transition state (2.02 Å of TS1c and 2.04 Å of TS1d).

The Pd-P1 bond lengths of cis- $[Pd(PPh_3)_2(Ph)Cl]$ and cis- $[Pd(PPh_3)_2(Ph)Br]$ are elongated to 2.51 and 2.50 Å, respectively, which are much longer than the Pd-P bonds in the

(20) (a) Amatore, C.; Pfluger, F. *Organometallics* **1990**, *9*, 2276-2282. (b) Evans, J.; O'Neill, L.; Kambhampati, V. L.; Rayner, G.; Turin, S.; Genge, A.; Dent, A. J.; Neisius, T. *J. Chem. Soc., Dalton Trans.* **2002**, 2207-2212.

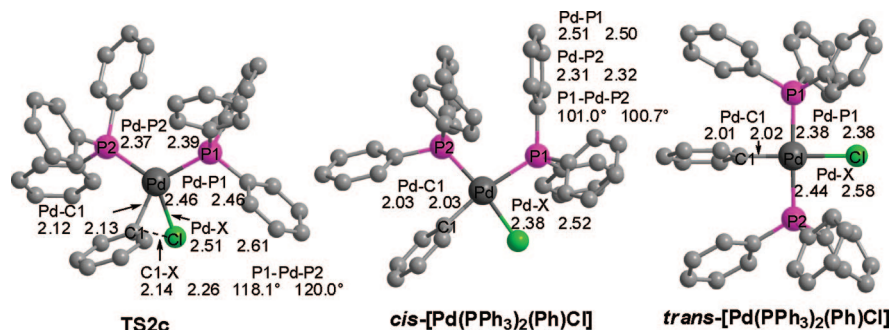


Figure 2. Geometries of species in path II with the PPh₃ ligand. The first number of bond lengths and angles belongs to PhCl, and the second belongs to PhBr.

monophosphine products **1c** and **1d**. The bond lengths of Pd–Cl of *cis*-[Pd(PPh₃)₂(Ph)Cl] and *cis*-[Pd(PPh₃)₂(Ph)Br] are also longer than those in **1c** and **1d**. The free energies of *cis*-[Pd(PPh₃)₂(Ph)Cl] and *cis*-[Pd(PPh₃)₂(Ph)Br] relative to [Pd(PPh₃)₂] are 6.9 and 1.5 kcal/mol, respectively (Table 3, entries 3 and 4). The *cis* products can isomerize to more stable *trans* products,²¹ which are exergonic by 9.3 and 8.8 kcal/mol for *trans*-[Pd(PPh₃)₂(Ph)Cl] and *trans*-[Pd(PPh₃)₂(Ph)Br], respectively.

3.4. Validation of the Gas-Phase-Optimized Geometries. The above calculations are based on geometries optimized in the gas phase because we hypothesize that the geometries in solution are the same as those in the gas phase. To justify this hypothesis, the key intermediates and transition states are fully optimized in the THF solution. The results show that the geometries change trivially after solution-phase optimization; i.e., bond lengths change by less than 0.07 Å and bond angles change by less than 5°²² (Figure 3). Furthermore, the Gibbs free energies also change only slightly. The barrier of TS1a increases 0.3 kcal/mol after optimization in the THF solution, and the barrier of TS1b becomes 1.0 kcal/mol higher than the gas-phase geometry (Table 4 entries 1 and 2). The free energy of TS1c is 1.9 kcal/mol higher than that of TS1a, which is very close to the corresponding gas-phase difference, 2.1 kcal/mol (Table 4, entry 3). Thus, both the structures and free energies are not sensitive to the geometry optimization method. Because gas-phase geometry optimization is much less CPU-demanding, we base our further discussions only on the gas-phase geometries.

4. Discussion

4.1. Comparison between Monophosphine and Bisphosphine Paths with the PPh₃ Ligand. When a multistep reaction reaches the steady state, the overall reaction barrier is approximately determined by the free-energy gap between the highest-energy species and the resting state.²³ The formation of the species with the highest free energy is the rate-determining step.²⁴ As to the two paths in the present study, it is evident that the path with the lowest free-energy maximum should be

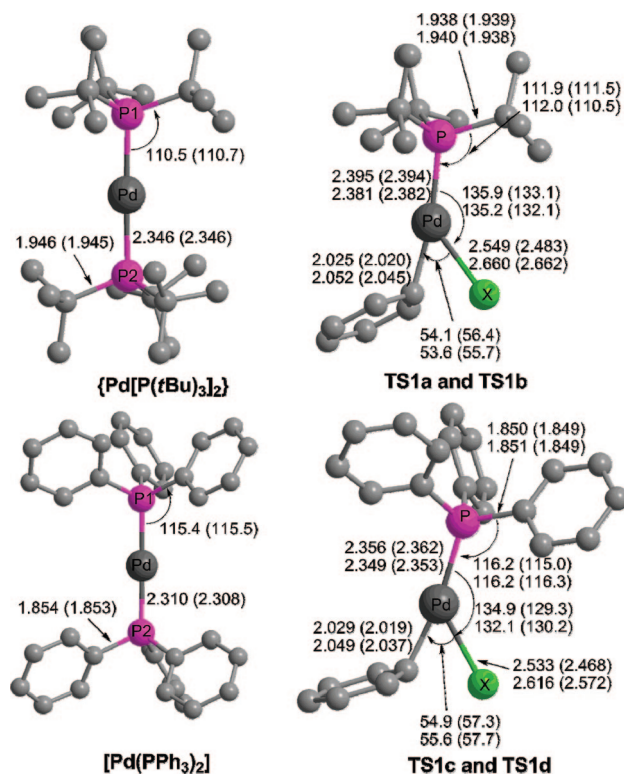


Figure 3. Geometry comparison of gas optimization and solution optimization. The first line of the values of bond lengths and angles belongs to the P(*t*Bu)₃ ligand, the second line belongs to the PPh₃ ligand, the first column belongs to PhCl, and the second column belongs to PhBr.

the favored path because the two paths have the same starting point [Pd(PR₃)₂].

In the case of PhCl, the highest-energy point of the monophosphine pathway is the oxidative addition transition state TS1c (Figure 4), and its free energy is 23.4 kcal/mol. On the other hand, the highest point of the bisphosphine pathway is the transition state TS2c, whose free energy is 34.4 and 11 kcal/mol higher than TS1c. As a result, if PhCl can undergo oxidative addition to Pd(PPh₃)₂, the monophosphine pathway must be the favored path. In this path, the oxidative addition via TS1c is the rate-determining step.

In the case of PhBr, the bisphosphine TS2d has a higher free energy than monophosphine TS1d again by 3 kcal/mol. Thus, the monophosphine path is still the favored path. In this path, [Pd(PPh₃)] becomes the highest-energy point instead of TS1d, indicating that the dissociation step is rate-determining where the dissociation energy is 22.0 kcal/mol (Figure 5). Note that all of the above results are consistent with the theoretical study

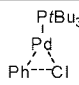
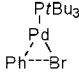
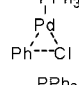
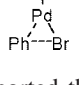
(21) Casado, A. L.; Espinet, P. *Organometallics* **1998**, *17*, 954–959.

(22) [Pd(PPh₃)₂] is optimized by PCM with UAHF radii to achieve convergence and has a minor negative frequency (–6 Hz) that cannot be eliminated through geometry optimization in the THF solution.

(23) Christmann, U.; Vilar, R. *Angew. Chem., Int. Ed.* **2005**, *44*, 366–374.

(24) We approximately equal the free-energy barrier to form {Pd[P(Ph₃)]} from {Pd[P(Ph₃)]₂} to the relative free energy of {Pd[P(Ph₃)]}. This assumption is based on the fact that the combination reaction of the ligand and coordination center in solution is controlled by diffusion and the equivalent barrier coming from the cage effect is only about 2 kcal/mol higher than the thermodynamic energy of the separated ligand and coordination center. Koenig, T. W.; Hay, B. P.; Finke, R. G. *Polyhedron* **1988**, *7*, 1499.

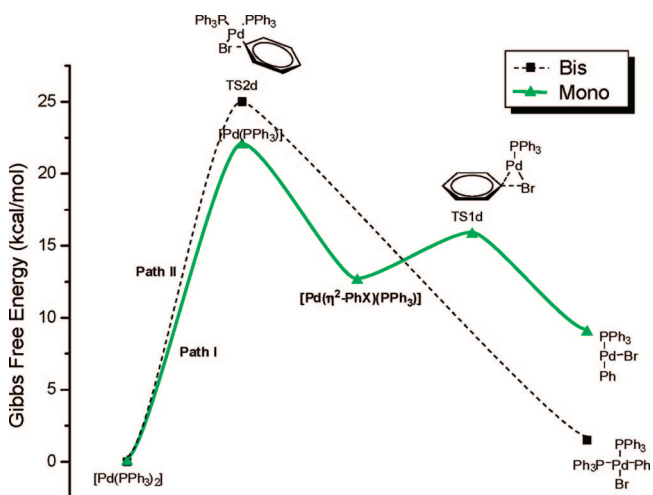
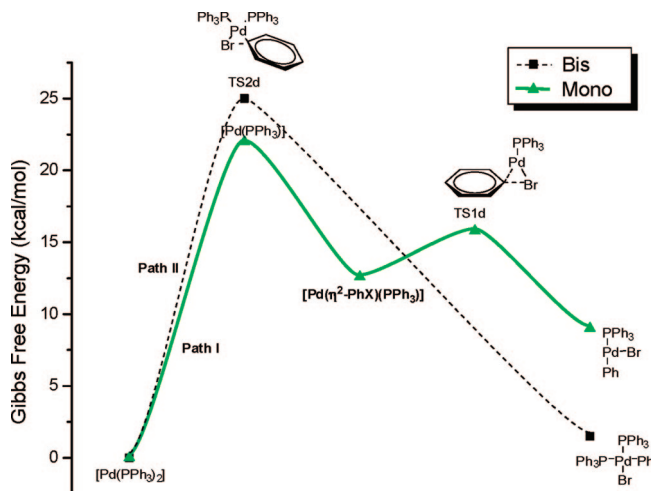
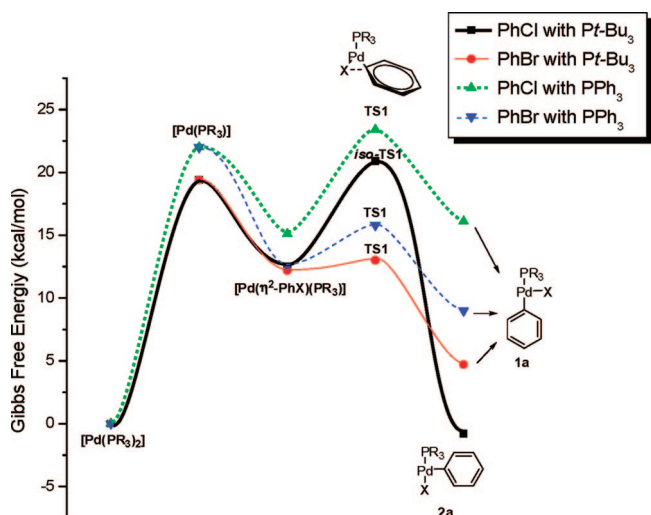
Table 4. Free Energies of TS1 for Geometries Fully Optimized in THF (kcal/mol)

Entry		G_2 (kcal/mol)	$\Delta G = G_2 - G_1$ (kcal/mol)
1		21.6	0.3
2		14.0	1.0
3		23.5	0.1
4		14.0	-1.8

of Lin et al., who reported that a monophosphine pathway is favored in the reaction of PhX with the model compound $\text{Pd}(\text{PMe}_3)_2$.²⁵

4.2. Reason That PtBu_3 Activates PhCl. Because both $\{\text{Pd}[\text{P}(\text{tBu})_3]_2\}$ and $[\text{Pd}(\text{PPh}_3)_2]$ can undergo oxidative addition via the monophosphine pathway, their different activities should originate from the difference between their monophosphine energy profiles. Figure 6 shows the free-energy profiles of path I. There are two uphill steps on the energy surface. The first step is ligand dissociation. Because the equilibrium between $[\text{PdL}_2]$ and $[\text{PdL}]$ is a fast step in the solution, the ligand dissociation energy actually reflects the concentration of monophosphine $[\text{PdPR}_3]$ in the reaction mixture. Because $\{\text{Pd}[\text{P}(\text{tBu})_3]\}$ has a dissociation energy 2.6 kcal/mol lower than $[\text{Pd}(\text{PPh}_3)]$, we can conclude that $\{\text{Pd}[\text{P}(\text{tBu})_3]\}$ has a much higher concentration in solution (ca. by 100-fold).

The second step is oxidative addition. The energy barriers of oxidative addition drawn in Figure 6 can be interpreted in two complementary ways: (1) The absolute energy height of TS1 determines whether the oxidative addition is rate-limiting. As for PhCl, both $\{\text{Pd}[\text{P}(\text{tBu})_3]\}$ and $[\text{Pd}(\text{PPh}_3)]$ have lower energies than TS1a, so that the overall rate is determined by oxidative addition for both $\{\text{Pd}[\text{P}(\text{tBu})_3]_2\}$ and $[\text{Pd}(\text{PPh}_3)_2]$. Moreover, the height of iso-TS1a is lower than that of TS1c by 2.5 kcal/mol, indicating that the overall addition rate of $\{\text{Pd}[\text{P}(\text{tBu})_3]_2\}$ with PhCl is faster by about 30 times that of

**Figure 4.** Energy profiles of monophosphine (solid green line, path I) and bisphosphine (dashed black line, path II) pathways of PhCl with $[\text{Pd}(\text{PPh}_3)_2]$.**Figure 5.** Energy profiles of monophosphine (solid green line) and bisphosphine (dashed black line) pathways of PhBr with $[\text{Pd}(\text{PPh}_3)_2]$.**Figure 6.** Free-energy profile of path I. The bold dashed line (green) indicates PhCl with a PPh_3 ligand, the bold line (black) PhCl with a PtBu_3 ligand, the dashed line (blue) PhBr with a PPh_3 ligand, and the plain line (red) PhBr with a PtBu_3 ligand.

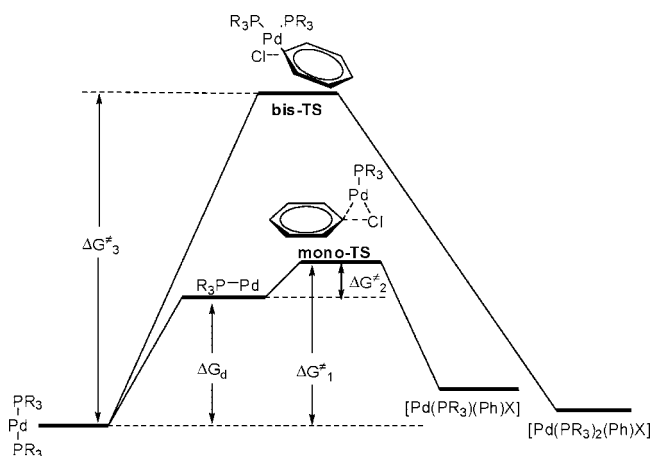
$[\text{Pd}(\text{PPh}_3)_2]$. (2) The relative free energy of TS1a or TS1c to $[\text{Pd}(\text{PR}_3)]$ reflects the difficulty of the oxidative addition of the monophosphine $[\text{Pd}(\text{PR}_3)]$. The relative energy of iso-TS1a to $\{\text{Pd}[\text{P}(\text{tBu})_3]\}$ is 1.5 kcal/mol, and this value is 1.4 kcal/mol for TS1c to $[\text{Pd}(\text{PPh}_3)_2]$. These two values are close to each other. Furthermore, $[\text{Pd}(\text{PPh}_3)]$ is even slightly more labile to oxidative addition than $\{\text{Pd}[\text{P}(\text{tBu})_3]\}$. Thus, it is the concentration of monophosphine Pd^0 that decides the rate of oxidative addition. This is consistent with experimental observation that the excess of phosphine ligands poisons the activity of catalysts.²⁶ Note that Norrby et al. also reported that the substantial part of the reaction barrier of oxidative addition came from the dissociation of one phosphine ligand.²⁷

4.3. Comparison of $\text{P}(\text{tBu})_3$ to Other Trialkylphosphine Ligands. In addition to PPh_3 , it is interesting to ask why other electron-donating ligands such as PMe_3 , PET_3 , and $\text{P}(\text{iPr})_3$ are

(25) Lam, K. C.; Marder, T. B.; Lin, Z. Y. *Organometallics* **2007**, *26*, 758.

(26) Beeby, A.; Bettington, S.; Fairlamb, I. J. S.; Goeta, A. E.; Kapdi, A. R.; Niemela, E. H.; Thompson, A. L. *New J. Chem.* **2004**, *28*, 600.

(27) Ahlquist, M.; Norrby, P.-O. *Organometallics* **2007**, *26*, 550.

Scheme 3. Oxidative Additions of [Pd(PR₃)₂] Complexes (R = Me, Et, *i*Pr, Ph, *t*Bu)

Table 5. Free-Energy Barriers of Oxidative Addition with PhCl and Dissociation Energies of Pd(PR₃)₂ (kcal/mol)

entry	Pd ⁰ complex	ΔG_d^\ddagger (kcal/mol)	ΔG_d (kcal/mol)	$\Delta G_2^\ddagger = \Delta G_1^\ddagger - \Delta G_d$ (kcal/mol)	ΔG_3^\ddagger (kcal/mol)
1	[Pd(PMe ₃) ₂]	24.6	26.0	-1.4	26.6
2	[Pd(PEt ₃) ₂]	23.2	22.4	0.8	30.4
3	[Pd(P <i>i</i> Pr ₃) ₂]	22.6	21.3	1.3	36.7
4	[Pd(P <i>t</i> Bu ₃) ₂]	20.9	19.4	1.5	
5	[Pd(PPh ₃) ₂]	23.4	22.0	1.4	34.4

not effective for the oxidative addition of PhCl to Pd⁰. To answer this question, we need to calculate the free-energy profiles of the oxidative addition of PhCl with [Pd(PR₃)₂] (R = Me, Et, *i*Pr; Scheme 3).

Because the associative displacement of one PR₃ ligand from Pd(PR₃)₂ leads to the key intermediate Pd(η^2 -PhCl)PR₃, it is warranted to check whether the substitution barrier decreases when changing PR₃ to a less bulky ligand, for example, PMe₃. The barrier of substitution of one PMe₃ by PhCl is 29.5 kcal/mol, and that by PhBr is 28.1 kcal/mol. These barriers are all much lower than that of TS3a or TS3b (Scheme 2), indicating that less steric repulsion lowers the barrier. However, the dissociation of PMe₃ from Pd(PMe₃)₂ is 26.0 kcal/mol. As a result, the direct dissociation of PMe₃ from Pd(PMe₃)₂ is more favored than the associative substitution.

The free energies of monophosphine transition states (ΔG_1^\ddagger), bisphosphine transition states (ΔG_3^\ddagger), and ligand dissociations relative to [Pd(PR₃)₂] (ΔG_d^\ddagger) are tabulated in Table 5. ΔG_1^\ddagger , the overall energy barrier of the monophosphine pathway of PMe₃, PEt₃, and P*i*Pr₃, is lower than the corresponding bisphosphine barrier, ΔG_3^\ddagger (Table 5, entries 1–3). Thus, the monophosphine pathway is also favored by these ligands. The case of PMe₃ is interesting (Table 5, entry 1), where the barrier of the monophosphine oxidative transition state (24.6 kcal/mol) with PhCl is a little lower than the dissociation energy of [Pd(PMe₃)₂] (26.0 kcal/mol). The barrier of the bisphosphine transition state of [Pd(PMe₃)₂] is only 26.6 kcal/mol, much lower than that of {Pd[P(*t*Bu)₃]₂} or [Pd(PPh₃)₂]. This indicates that PMe₃ is not a good model to simplify P*t*Bu₃ or PPh₃ in the computational study of Pd catalysis. In a related study, Buchwald et al. also found that the use of smaller 2-phosphino-2',6'-dimethoxybiphenyl to replace the more bulky 2-dicyclohexy-

lphosphino-2',6'-dimethoxybiphenyl ligand resulted in inaccurate relative energies.²⁸

Compared to the dissociation energy of P*t*Bu₃ (i.e., 19.4 kcal/mol), [Pd(PMe₃)₂], [Pd(PEt₃)₂], and [Pd(P(*i*Pr)₃)₂] each has a higher dissociation free energy of 26.0, 22.4, and 21.3 kcal/mol, respectively (Table 5, column 3). This trend is similar to the case of the palladium N-heterocyclic carbene complexes.²⁹ Thus, the concentrations of monophosphine [PdPR₃] (R = Me, Et, *i*Pr) are much lower than that of {Pd[P(*t*Bu)₃]}. The fourth column in Table 5 shows the relative energy of the monophosphine transition state to [PdPR₃] (ΔG_2^\ddagger ; Scheme 3). The relative energy barriers of PMe₃, PEt₃, and P(*i*Pr)₃ with PhCl are all less than 2 kcal/mol and even lower than those of P(*t*Bu)₃ and PPh₃. This means that the activities of monophosphine species [PdPMe₃], [PdPEt₃], and [PdP(*i*Pr)₃] are even higher than that of P(*t*Bu)₃ or PPh₃. However, their concentrations are too low to make them useful in catalytic cross-coupling reactions.

5. Conclusion

Here we employ DFT methods with the PCM model to study the mechanism of oxidative addition of PhCl and PhBr to [Pd(PR₃)₂] (R = Me, Et, *i*Pr, *t*Bu, Ph). The following conclusions can be drawn from our calculations:

(1) For both PhCl and PhBr, the transition states of oxidative addition to [Pd(PPh₃)₂] have much higher free energies than the monophosphine transition states. The bisphosphine transition state of {Pd[P(*t*Bu)₃]₂} does not even exist. Thus, both {Pd[P(*t*Bu)₃]₂} and [Pd(PPh₃)₂] perform oxidative additions via a monophosphine pathway with PhX. Although the dissociation of one phosphine ligand is endergonic, the 12-electron monophosphine species [PdPR₃] is the most active species to oxidative addition.

(2) Among different PR₃ ligands (R = Me, Et, *i*Pr, *t*Bu, Ph), the free-energy barriers for the oxidative addition to PdPR₃ do not change significantly (i.e., less than 2 kcal/mol). This gives rise to an important question, why is P(*t*Bu)₃ the only catalytically active ligand toward aryl chlorides among the above five ligands? Through calculations, the possible reason is found to be that the dissociation energy of P(*t*Bu)₃ from {Pd[P(*t*Bu)₃]₂} is significantly lower than that of [Pd(PR₃)₂] (where R = Me, Et, *i*Pr, Ph). Thus, it is proposed that the difference of the dissociation energies from PdL₂ to PdL and L (L = ligand) between the various PR₃ ligands governs their different reactivity in the oxidative addition.

Acknowledgment. This study was supported by the National Natural Science Foundation of China (Grant 20602034), the Anhui Provincial Natural Science Foundation (Grant 070416237), and the Excellent Young Scholars Foundation of Anhui Province (Grant 08040106829). We also thank the USTC-HP, Wuxi, and Shanghai Supercomputer Center for the computational resources.

Supporting Information Available: Detailed optimized geometries and free energies. This material is available free of charge via the Internet at <http://pubs.acs.org>.

OM701065F

(28) Barder, T. E.; Biscoe, M. R.; Buchwald, S. L. *Organometallics* **2007**, *26*, 2183.

(29) Green, J. C.; Herbert, B. J.; Lonsdale, R. J. *Organomet. Chem.* **2005**, *690*, 6054.